Available online at www.sciencedirect.com

ScienceDirect

Ceramics International 41 (2015) 10531–10536

CERAMICS INTERNATIONAL

www.elsevier.com/locate/ceramint

$5ZnO \cdot 2B_2O_3$–$Pb_{1.5}Nb_2O_{6.5}$ microwave dielectric ceramics with near-zero temperature coefficient of resonant frequency

Yunxiang Hu[a], Ze Jin[a], Qiuyun Fu[a,b,*], Dongxiang Zhou[a], Zhiping Zheng[a], Wei Luo[a], Jun Zhao[a]

[a]School of Optical and Electronic Information, Huazhong University of Science and Technology, Wuhan 430074, China

[b]State Key Laboratory of Material Processing and Die & Mould Technology, Huazhong University of Science and Technology, Wuhan 430074, China

Received 19 March 2015; received in revised form 20 April 2015; accepted 25 April 2015

Available online 5 May 2015

Abstract

The effects of $Pb_{1.5}Nb_2O_{6.5}$ addition were investigated on the densification, phase evolution, microstructure, and microwave dielectric properties of $5ZnO \cdot 2B_2O_3$ ceramics. It was shown that a 5.5 mol% addition of $Pb_{1.5}Nb_2O_{6.5}$ to $5ZnO \cdot 2B_2O_3$ ceramics successfully tailored its temperature coefficient of resonant frequency (τ_f) from -80 to ~ 0 ppm/°C and lowered its sintering temperature from 955 to 890 °C without degrading its microwave dielectric properties. $5ZnO \cdot 2B_2O_3$ ceramics sintered at 890 – 910 °C for 3 h with 5.0 – 6.0 mol% $Pb_{1.5}Nb_2O_{6.5}$ additions exhibited excellent microwave dielectric properties: $\varepsilon_r = 7.8 - 8.3$, $Q \times f = 11{,}500 - 15{,}200$ GHz, and -9.2 ppm/°C $\leq \tau_f \leq +6.6$ ppm/°C @ ~ 7.4 GHz. The ceramics showed cofiring compatibility with Ag and were therefore novel candidates for LTCC substrates.

Keywords: Near-zero temperature coefficient of resonant frequency; Microwave dielectric properties; $5ZnO \cdot 2B_2O_3$ ceramics; $Pb_{1.5}Nb_2O_{6.5}$; LTCC substrates

1. Introduction

With the rapid growth of mobile and wireless telecommunication system in the consumer electronic market, the low-temperature cofired ceramic (LTCC) technology is playing an important role in the development of various electronic modules. By the LTCC technology, ceramic dielectric substrates and low-melting metallic conductors are stacked and cofired in multilayers in special patterns to fulfill different electrical functions. Generally ceramic substrates are required to have a low relative permittivity ($\varepsilon_r \sim 4$–9) to shorten the delay time of the transmitted signals, a high quality factor ($Q \times f > 10{,}000$ GHz) to decrease the transmission loss, and a near-zero temperature coefficient of resonant frequency (-10 ppm/°C $< \tau_f < +10$ ppm/°C) to ensure the thermal stability. In addition, substrates must have a sintering temperature lower than the melting point of the conductor such as Ag (961 °C) and be chemically compatible with the conductor during cofiring [1].

In addition to the traditional glass + ceramics [2] and glass–ceramics [3] systems, some borate [4,5] and molybdate [6] ceramics with originally low sintering temperature have been recently investigated for LTCC substrates. In our previous work [7], we reported that $5ZnO \cdot 2B_2O_3$ (also described as a phase with the composition $3ZnO \cdot B_2O_3$ [7–9]) ceramic sintered in air at 955 °C for 1 h exhibited good microwave dielectric properties: $\varepsilon_r \sim 6.9$, $Q \times f \sim 20{,}647$ GHz (@ 6.35 GHz) and $\tau_f \sim -80$ ppm/°C and was proposed as a substrate candidate. However, the large negative τ_f value puts constraints on their application in LTCC substrates and needs to be tailored to a near-zero value to prevent the disturbance from temperature variation.

A near-zero τ_f value was usually obtained by using two components with opposite τ_f values in many ceramic systems, such as $CaWO_4$–TiO_2 [10], Zn_2TiO_4–TiO_2 [11], $NiNb_2O_6$–TiO_2 [12], Bi_2MoO_6–TiO_2 [13], $MgWO_4$–$CaTiO_3$ [14], Zn_2SiO_4–$CaTiO_3$ [15], and Mg_2SiO_4–$CaTiO_3$ [16] ceramic systems, where both TiO_2 and $CaTiO_3$ were of large positive τ_f values. Since $5ZnO \cdot 2B_2O_3$ ceramic has a negative τ_f value, a component with a large positive τ_f value should be added to tailor its τ_f value. We found unfortunately that both TiO_2 and $CaTiO_3$ were not suitable

*Corresponding author. Tel.: +86 27 8755 8482.
E-mail address: fuqy@mail.hust.edu.cn (Q. Fu).

http://dx.doi.org/10.1016/j.ceramint.2015.04.146
0272-8842/

to fulfill this function for titanates reacted with zinc borates [17,18]. However it was reported that $Pb_{1.5}Nb_2O_{6.5}$ had a τ_f of +1239 ppm/°C [19,20]. Therefore it is logical to speculate that the $(100-x)$ mol% $5ZnO \cdot 2B_2O_3 - x$ mol% $Pb_{1.5}Nb_2O_{6.5}$ ceramic composites have adjustable τ_f values depending on different x.

This present paper aimed to tailor the τ_f value of $5ZnO \cdot 2B_2O_3$ ceramics to near zero by the addition of $Pb_{1.5}Nb_2O_{6.5}$. Effects of the $Pb_{1.5}Nb_2O_{6.5}$ addition on the sintering behavior, ε_r, and $Q \times f$ of the ceramics were also investigated in detail. To our best knowledge, no papers reported on the adjustment of τ_f of $5ZnO \cdot 2B_2O_3$ ceramics.

2. Experimental procedure

Both the $5ZnO \cdot 2B_2O_3$ and $Pb_{1.5}Nb_2O_{6.5}$ powders were synthesized by the conventional solid-state reaction route. Chemical powders of ZnO (≥99.7%) and H_3BO_3 (≥99.5%) were weighed in a composition of $5ZnO \cdot 2B_2O_3$, dry mixed thoroughly using mortar and pestle, and then calcined at 750 °C for 1 h to form the $5ZnO \cdot 2B_2O_3$ powder. The powder X-ray diffraction (XRD) result (not shown) confirmed that the synthesized $5ZnO \cdot 2B_2O_3$ powder was almost comprised of $3ZnO \cdot B_2O_3$ phase (JCPDS 71-2063). AR grade oxide PbO (≥99.0%) and high purity chemical of Nb_2O_5 (99.99%) were weighed in a molar ratio of 1.5 to 1, agate ball milled with deionized water for 4 h, dried, and then calcined in a closed Al_2O_3 crucible at 750 °C for 4 h to synthesize the $Pb_{1.5}Nb_2O_{6.5}$ powder [20]. The powder XRD result (not shown) confirmed that the synthesized $Pb_{1.5}Nb_2O_{6.5}$ powder was almost pure $Pb_{1.5}Nb_2O_{6.5}$ phase (JCPDS 72-1492).

The $5ZnO \cdot 2B_2O_3 - Pb_{1.5}Nb_2O_{6.5}$ ceramics were prepared using the obtained $5ZnO \cdot 2B_2O_3$ and $Pb_{1.5}Nb_2O_{6.5}$ powders. These two powders were weighed in a composition of $(100-x)$ mol% $5ZnO \cdot 2B_2O_3 - x$ mol% $Pb_{1.5}Nb_2O_{6.5}$ (x=4.5–7.0), agate ball milled with deionized water for 1 h, and dried. The dried mixtures were pelletized well with an aqueous polyvinyl alcohol (PVA) solution as a binder, and bilaterally pressed into cylindrical disks of 25 mm in diameter and about 12.5 mm in height under a pressure of 50 MPa. The compacts were sintered at 870–930 °C for 3 h in air. For the test of cofiring compatibility with Ag, several small disk compacts were sintered at 890 °C for 3 h in air using the 94.5 mol% $5ZnO \cdot 2B_2O_3$–5.5 mol% $Pb_{1.5}Nb_2O_{6.5}$ mixture powder with an extra 20 wt% Ag_2O powder.

The bulk densities of sintered specimens were measured by the Archimedes method. The crystalline phases of sintered samples were identified with an X-ray diffractometer (XRD-7000, Shimadzu Corporation, Japan) using a CuKα radiation having a wavelength of 1.5406 Å within 2θ range of 10–70°. The microstructures were examined by a scanning electron microscope (SEM, VEGA3 TESCAN). The element contents were identified by an energy dispersive spectrometer (EDS, OXFORD X-Max). ε_r and $Q \times f$ were measured by the Hakki–Coleman dielectric resonator method using an Agilent network analyzer (E5071C) [21]. τ_f was measured by the same method, but with the resonator placed into a thermostat. The test temperature ranged from 30 to 80 °C and τ_f was calculated as follows:

$$\tau_f = \frac{(f_{80} - f_{30}) \times 10^6}{f_{30}(80-30)} \quad (\text{ppm}/^\circ\text{C}) \tag{1}$$

where f_{80} and f_{30} are the resonant frequencies at 80 and 30 °C, respectively.

3. Results and discussion

Fig. 1 shows the XRD patterns of $5ZnO \cdot 2B_2O_3$ ceramics sintered at different temperatures for 3 h with a 5.5 mol% $Pb_{1.5}Nb_2O_{6.5}$ addition. In all ceramics sintered at 870–930 °C, the principal crystalline phase was considered to be $3ZnO \cdot B_2O_3$ (JCPDS 71-2063, monoclinic), the added $Pb_{1.5}Nb_2O_{6.5}$ phase in

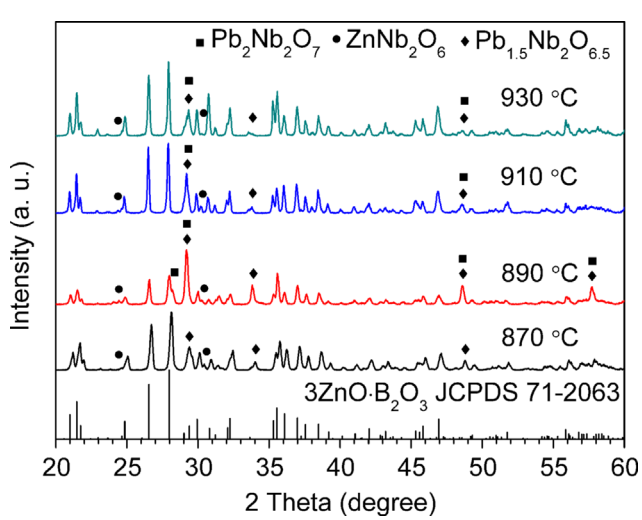

Fig. 1. XRD patterns of $5ZnO \cdot 2B_2O_3$ ceramics sintered at different temperatures for 3 h with a 5.5 mol% $Pb_{1.5}Nb_2O_{6.5}$ addition.

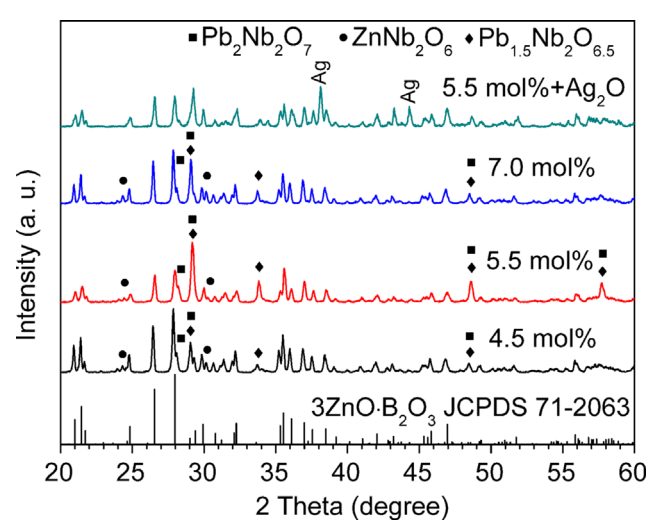

Fig. 2. XRD patterns of $5ZnO \cdot 2B_2O_3$ ceramics sintered at 890 °C for 3 h with different $Pb_{1.5}Nb_2O_{6.5}$ additions.

green bodies was still detected as a secondary crystalline phase, and a trace $ZnNb_2O_6$ (JCPDS 76-1827, orthorhombic) phase, which might result from the partial reaction between the $5ZnO \cdot 2B_2O_3$ and $Pb_{1.5}Nb_2O_{6.5}$ powders, was also detected. In addition, when the sintering temperature rose up to 890 °C, a $Pb_2Nb_2O_7$ (JCPDS 43-0960, hexagonal) phase formed. Furthermore, the diffraction peak intensities of the $Pb_{1.5}Nb_2O_{6.5}$ and $Pb_2Nb_2O_7$ phases decreased with increasing sintering temperature in the range of 890–930 °C, and this might result from the partial volatilization of these two phases at higher temperatures in comparison with the SEM, density, and sintering shrinkage observations mentioned below.

Fig. 2 shows the XRD patterns of $5ZnO \cdot 2B_2O_3$ ceramics sintered at 890 °C for 3 h with different contents of $Pb_{1.5}Nb_2O_{6.5}$. It can be seen that the principal crystalline phase in ceramics with 4.5–7.0 mol% $Pb_{1.5}Nb_2O_{6.5}$ additions was all $3ZnO \cdot B_2O_3$, indicating that the addition of $Pb_{1.5}Nb_2O_{6.5}$ did not change the principal phase in ceramics. In these ceramics, the secondary phases included the $Pb_{1.5}Nb_2O_{6.5}$ and $Pb_2Nb_2O_7$ phases, and a trace $ZnNb_2O_6$ phase was detected. For comparison, Fig. 2 also shows the XRD pattern of the 94.5 mol% $5ZnO \cdot 2B_2O_3$–5.5 mol% $Pb_{1.5}Nb_2O_{6.5}$ ceramics cofired with an extra 20 wt% Ag_2O at 890 °C for 3 h. It was found that no Ag-containing compounds were detected except for the Ag phase.

Fig. 3 shows the SEM images of $5ZnO \cdot 2B_2O_3$ ceramics sintered at 870–930 °C for 3 h with a 5.5 mol% $Pb_{1.5}Nb_2O_{6.5}$ addition. It is clear that sintering temperature had a significant influence on the microstructure of ceramics. Samples sintered at 870 °C were porous with small and uniform grains bound together (Fig. 3a). When the sintering temperature rose up to 890 °C, ceramics became dense with large grains (Fig. 3b). Abnormal grain growth for $3ZnO \cdot B_2O_3$ grains was observed and some grains grew up to 20 μm in size. Some rod grains formed which were attributed to the $Pb_2Nb_2O_7$ phase based on EDS and XRD results. In addition some glassy lumps were

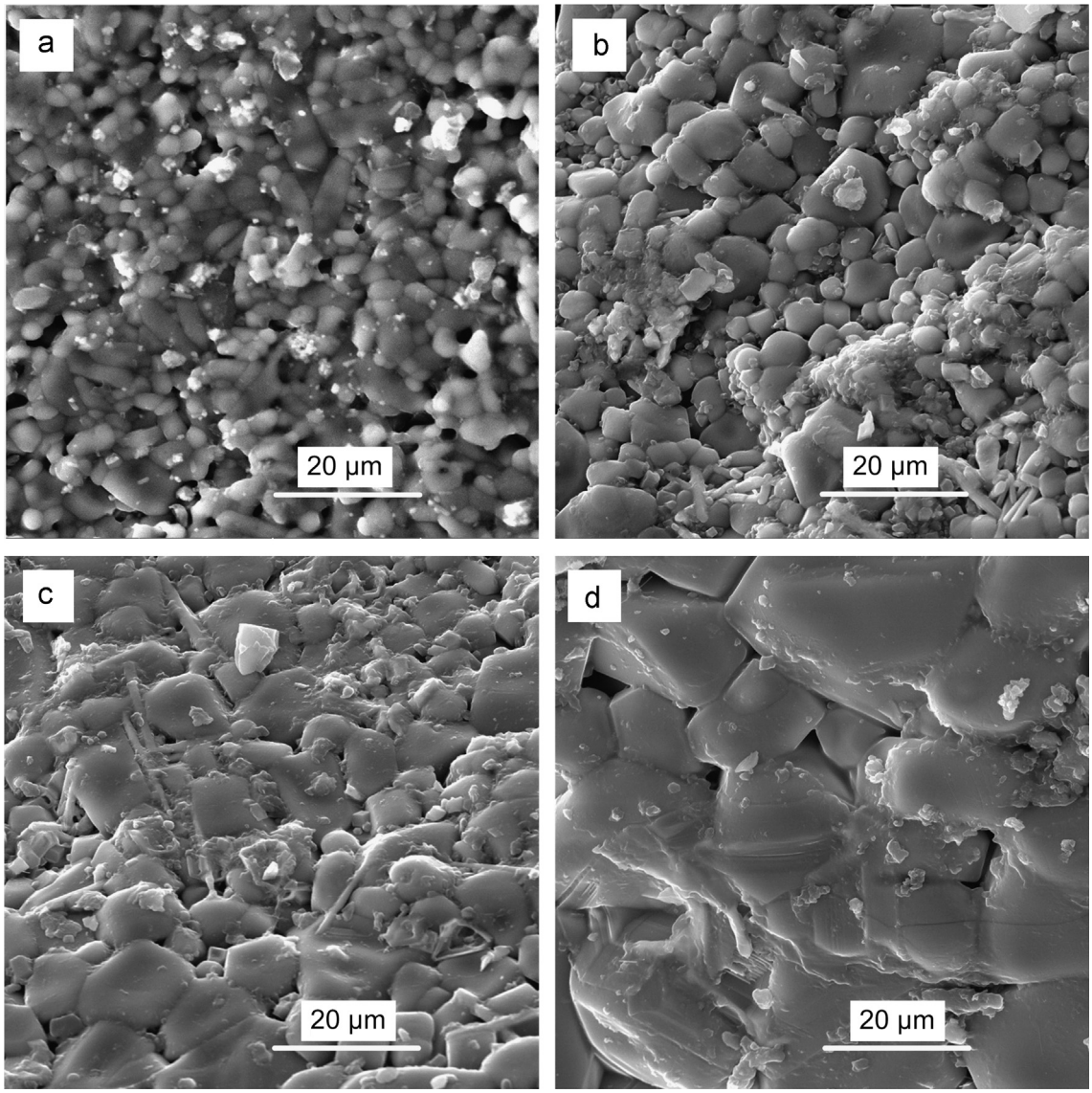

Fig. 3. SEM images of $5ZnO \cdot 2B_2O_3$ ceramics sintered for 3 h with a 5.5 mol% $Pb_{1.5}Nb_2O_{6.5}$ addition at different temperatures: (a) 870, (b) 890, (c) 910, and (d) 930 °C.

evidently observed in ceramics (Fig. 3b) and EDS showed they contained Zn, Pb, O, and B. The formation of this glass might be responsible for the densification of ceramics with $Pb_{1.5}Nb_2O_{6.5}$ addition at a much lower temperature (890 °C) than without $Pb_{1.5}Nb_2O_{6.5}$ addition [7]. Furthermore, as temperature rose further up to 910 and 930 °C, the $3ZnO \cdot B_2O_3$ grains grew larger and larger, and the number of $Pb_2Nb_2O_7$ rods in ceramics became less and less due to their volatilization (Fig. 3c and d).

Fig. 4 shows the SEM images of $5ZnO \cdot 2B_2O_3$ ceramics sintered at 890 °C for 3 h with different $Pb_{1.5}Nb_2O_{6.5}$ additions. The microstructures of ceramics with 4.5–7.0 mol% additions almost remained unchanged except that there were more rods in ceramics with higher additions (Fig. 4a–c). For comparison, Fig. 4d shows an SEM image of the 94.5 mol% $5ZnO \cdot 2B_2O_3$–5.5 mol% $Pb_{1.5}Nb_2O_{6.5}$ ceramics cofired with an extra 20 wt% Ag_2O at 890 °C for 3 h. It is evident that cofiring produced a new Ag phase and did not affect the morphologies and distributions of various phases in ceramics. In combination with the XRD result in Fig. 2, therefore, it is sound to conclude that $5ZnO \cdot 2B_2O_3$–$Pb_{1.5}Nb_2O_{6.5}$ ceramics exhibited a good chemical compatibility with Ag electrodes during cofiring.

Fig. 5 shows the bulk density and linear shrinkage of $5ZnO \cdot 2B_2O_3$ ceramics with various $Pb_{1.5}Nb_2O_{6.5}$ additions as a function of sintering temperature. All ceramics with 4.5–7.0 mol% additions exhibited a similar variation in bulk density (linear shrinkage) with increasing sintering temperature. As sintering temperature rose up from 870 to 890 °C, the bulk density and linear shrinkage both increased dramatically, which was attributed to the liquid-phase sintering of the formed ZnO–PbO–B_2O_3 liquid. As sintering temperature rose further up from 890 to 900 °C, they both reached a plateau of circa 4.06 g/cm^3 (96% of the theoretical density, 4.24 g/cm^3, of the $3ZnO \cdot B_2O_3$ phase from JCPDS data) and 20.6%, respectively. Clearly, the addition of $Pb_{1.5}Nb_2O_{6.5}$ greatly lowered the densification temperature of $5ZnO \cdot 2B_2O_3$ ceramics from

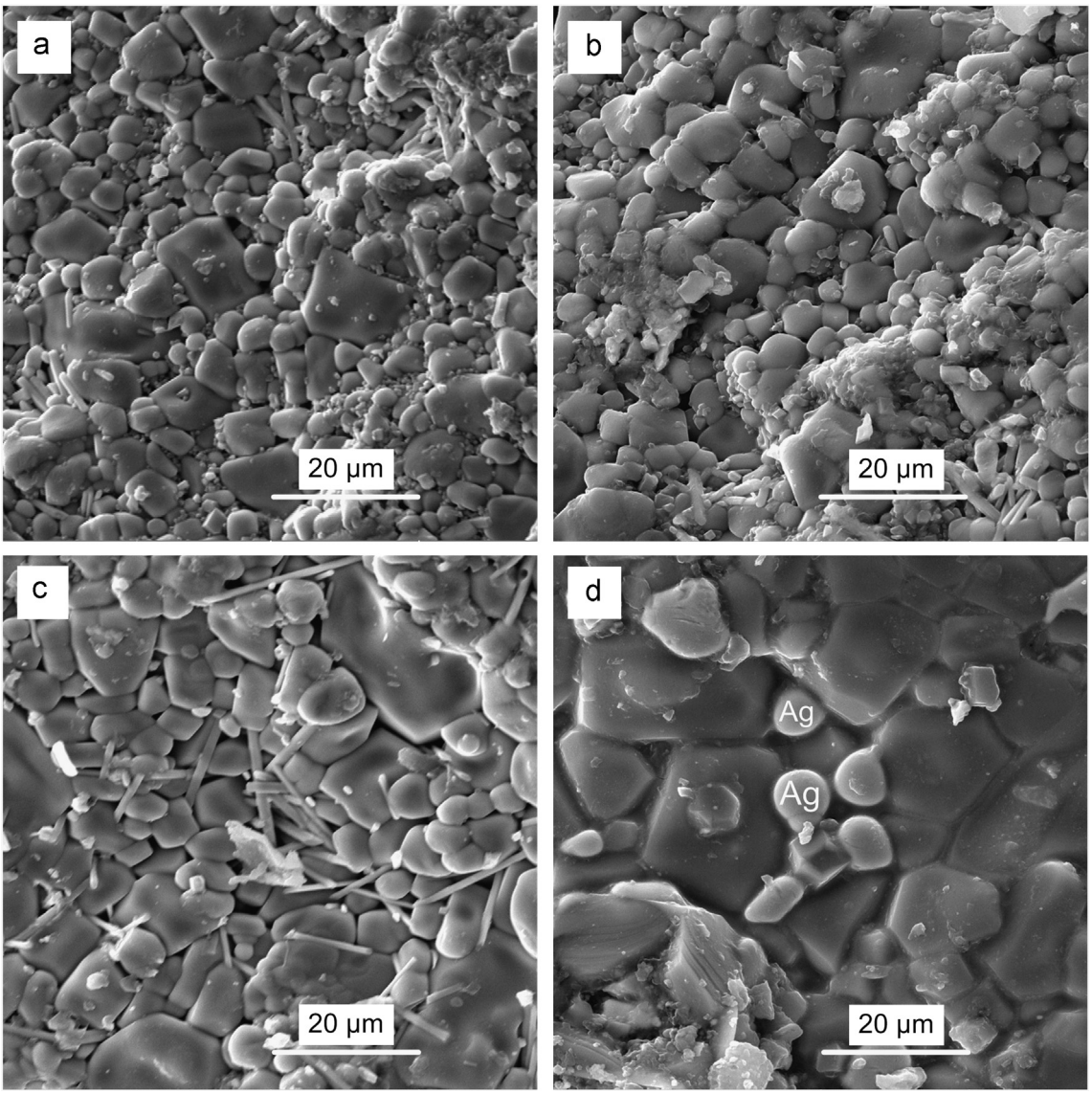

Fig. 4. SEM images of $5ZnO \cdot 2B_2O_3$ ceramics sintered at 890 °C for 3 h with various $Pb_{1.5}Nb_2O_{6.5}$ additions: (a) 4.5 mol%, (b) 5.5 mol%, (c) 7.0 mol%, and (d) 5.5 mol%+extra 20 wt% Ag_2O.

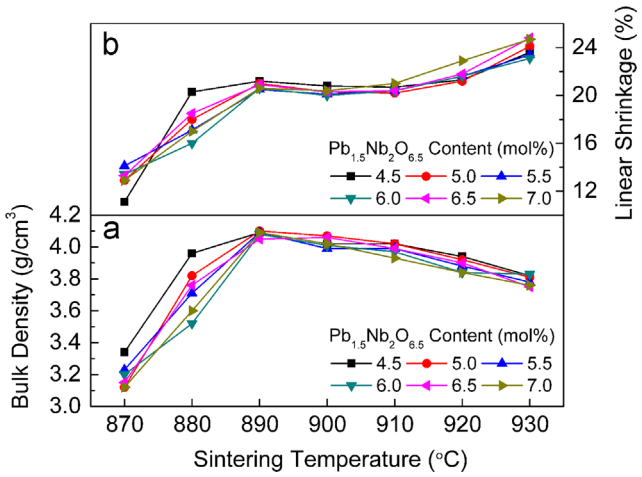

Fig. 5. (a) Bulk density and (b) linear shrinkage of $5ZnO \cdot 2B_2O_3$ ceramics sintered for 3 h with various $Pb_{1.5}Nb_2O_{6.5}$ additions as a function of sintering temperature.

955 to 890 °C [7]. With the further rise in sintering temperature from 900 to 930 °C, the density slightly decreased while the shrinkage slightly increased, indicating a ceramic mass loss in this temperature range. In combination with XRD and SEM results, this mass loss was attributed to the partial volatilization of the $Pb_{1.5}Nb_2O_{6.5}$ and $Pb_2Nb_2O_7$ phases in ceramics at higher temperatures than 900 °C. Finally, for ceramics sintered at 890–900 °C for 3 h, the $Pb_{1.5}Nb_2O_{6.5}$ addition in the range of 4.5–7.0 mol% had little influence on the density and shrinkage of ceramics.

Fig. 6 illustrates ε_r and $Q \times f$ of $5ZnO \cdot 2B_2O_3$ ceramics with various $Pb_{1.5}Nb_2O_{6.5}$ additions as a function of sintering temperature. It can be seen that at a fixed addition, ε_r vs. sintering temperature had a similar trend to density vs. sintering temperature, while $Q \times f$ vs. sintering temperature to shrinkage vs. sintering temperature. Remarkable increases in ε_r and $Q \times f$ took place in the sintering temperature range from 870 to 890 °C, and this was due to the removal of pores and the densification of ceramics. In the range of 890 − 900 °C, both ε_r and $Q \times f$ reached a plateau. Then for the high sintering temperature stage from 900 to 930 °C, ε_r slightly decreased as a result of the slight decrease in the density and the partial volatilization of the $Pb_{1.5}Nb_2O_{6.5}$ ($\varepsilon_r = 259$, $Q \times f = 3015$ GHz) and $Pb_2Nb_2O_7$ ($\varepsilon_r = 158$, $Q \times f = 4050$ GHz) phases which have a much higher ε_r than the $3ZnO \cdot B_2O_3$ ($\varepsilon_r = 6.9$, $Q \times f = 20{,}647$ GHz) main phase, while $Q \times f$ slightly increased since the $3ZnO \cdot B_2O_3$ main phase has a much high $Q \times f$ over those two partially volatilized lead niobates [7,19,20]. Finally, for ceramics sintered at 890–900 °C for 3 h, the $Pb_{1.5}Nb_2O_{6.5}$ addition in the range of 4.5–7.0 mol% had a slight influence on ε_r and $Q \times f$ of ceramics. As expected, ε_r slightly increased while $Q \times f$ decreased with increasing addition. This was mainly because the added $Pb_{1.5}Nb_2O_{6.5}$ presented in sintered ceramics in the form of the $Pb_{1.5}Nb_2O_{6.5}$ and $Pb_2Nb_2O_7$ phases, both of which have a much higher ε_r and a much lower $Q \times f$ than the $3ZnO \cdot B_2O_3$ main phase.

Fig. 7 shows τ_f value of $5ZnO \cdot 2B_2O_3$ ceramics sintered at different temperatures for 3 h as a function of $Pb_{1.5}Nb_2O_{6.5}$ addition. It is obvious that for all samples sintered at 870–920 °C τ_f shifted towards the positive direction with increasing $Pb_{1.5}Nb_2O_{6.5}$ addition. This shift should be related to the presence of the $Pb_{1.5}Nb_2O_{6.5}$ phase and the formation of the $Pb_2Nb_2O_7$ phase in ceramics, since these two phases have a positive τ_f value of circa +1239 ppm/°C and +814 ppm/°C, respectively [19,20]. In particular, it is worth to pointing out that for ceramics sintered at 890 °C the τ_f value was well linear with the $Pb_{1.5}Nb_2O_{6.5}$ addition x. Based on the 6 experimental point data in Fig.7, the Origin software gave a linear regression equation of τ_f in ppm/°C on x in mol% with Adj. R-Square = 0.98395:

$$\tau_f = -64.1219 + 11.93714x. \quad (2)$$

When $x = 0$ mol%, from this equation we have $\tau_f = -64.1219$ ppm/°C. This τ_f value is quite close to the reported one of $5ZnO \cdot 2B_2O_3$ ceramics without the $Pb_{1.5}Nb_2O_{6.5}$ addition [7]. When $x = 100$ mol%, we have $\tau_f = +1129.5921$ ppm/°C, which is in between the two τ_f values of $Pb_2Nb_2O_7$ and $Pb_{1.5}Nb_2O_{6.5}$ ceramics [19,20].

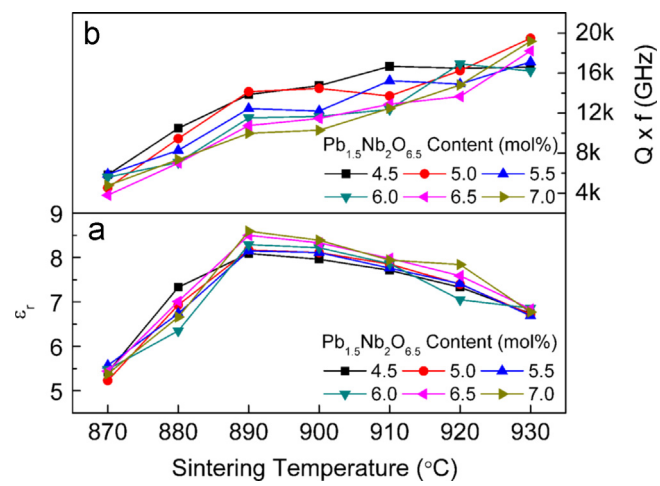

Fig. 6. (a) ε_r and (b) $Q \times f$ of $5ZnO \cdot 2B_2O_3$ ceramics sintered for 3 h with various $Pb_{1.5}Nb_2O_{6.5}$ additions as a function of sintering temperature.

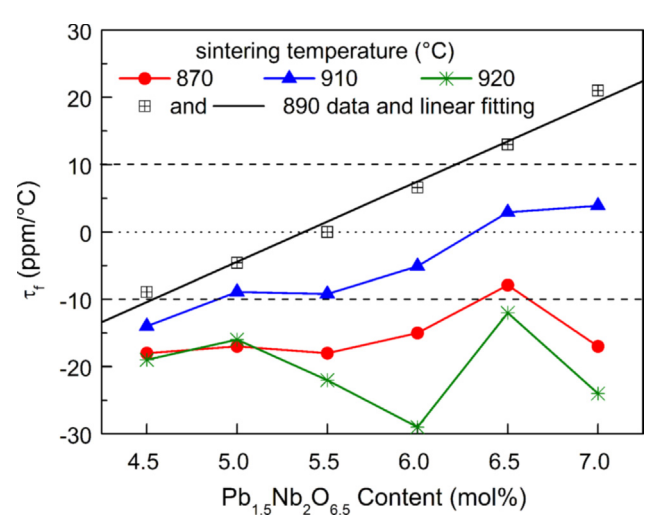

Fig. 7. τ_f of $5ZnO \cdot 2B_2O_3$ ceramics sintered at different temperatures for 3 h as a function of $Pb_{1.5}Nb_2O_{6.5}$ addition.

On the other hand, it can be seen from Fig. 7 that the sintering temperature had a great effect on the τ_f value of ceramics with a fixed $Pb_{1.5}Nb_2O_{6.5}$ addition. Those τ_f vs. x curves for other sintering temperatures were all below the one for 890 °C. Ceramics sintered at 870 °C had a lower τ_f than at 890 °C due to the lack of the $Pb_2Nb_2O_7$ phase and presence of many pores in ceramics. At a fixed $Pb_{1.5}Nb_2O_{6.5}$ addition, when sintering temperature was higher than 890 °C, the τ_f value of ceramics decreased due to the partial volatilization of the $Pb_2Nb_2O_7$ and $Pb_{1.5}Nb_2O_{6.5}$ phases at higher temperatures.

Finally, in order to obtain ceramics with -10 ppm/°C $\leq \tau_f \leq +10$ ppm/°C, based on Fig. 7 we suggest an optimal $Pb_{1.5}Nb_2O_{6.5}$ addition range of 5.0–6.0 mol% and an optimal sintering temperature range of 890–910 °C. As a result, $5ZnO \cdot 2B_2O_3$ ceramics sintered at 890–910 °C for 3 h with 5.0–6.0 mol% $Pb_{1.5}Nb_2O_{6.5}$ additions were dense and exhibited excellent microwave dielectric properties: $\varepsilon_r = 7.8$–8.3, $Q \times f = 11{,}500$–15,200 GHz, and -9.2 ppm/°C $\leq \tau_f \leq +6.6$ ppm/°C @ ~7.4 GHz.

4. Conclusions

The sintering behavior and microwave dielectric properties of $5ZnO \cdot 2B_2O_3$ ceramics with $Pb_{1.5}Nb_2O_{6.5}$ additions were studied in this work. It was found that the addition of $Pb_{1.5}Nb_2O_{6.5}$ greatly affected the densification, phase evolution, and microwave dielectric properties of ceramics. Sintering compositions of $(100-x)$ mol% $5ZnO \cdot 2B_2O_3 - x$ mol% $Pb_{1.5}Nb_2O_{6.5}$ ($x = 5.0$–6.0) at 890–910 °C in air for 3 h gave dense ceramics with excellent microwave dielectric properties: $\varepsilon_r = 7.8-8.3$, $Q \times f =$ 11,500–15,200 GHz, and -9.2 ppm/°C $\leq \tau_f \leq +6.6$ ppm/°C @ ~7.4 GHz. The $Pb_{1.5}Nb_2O_{6.5}$ addition not only tailored the τ_f value to ~0 ppm/°C but also lowered the sintering temperature of the ceramics. Moreover, the ceramics had a chemical compatibility with Ag during cofiring, indicating they are promising candidates for LTCC substrates.

References

1 M.T. Sebastian, H. Jantunen, Low loss dielectric materials for LTCC applications: a review, Int. Mater. Rev. 53 (2) (2008) 57–90.

2 Y. Imanaka, N. Kamehara, K. Niwa, The Sintering process of glass/alumina composites, J. Ceram. Soc. Jpn. 98 (8) (1990) 812–816.

3 C.R. Chang, J.H. Jean, Crystallization kinetics and mechanism of low-dielectric, low-temperature, cofirable $CaO–B_2O_3–SiO_2$ glass–ceramics, J. Am. Ceram. Soc. 82 (7) (1999) 1725–1732.

4 M. Ohashi, H. Ogawa, A. Kan, E. Tanaka, Microwave dielectric properties of low-temperature sintered $Li_3AlB_2O_6$ ceramic, J. Eur. Ceram. Soc. 25 (2005) 2877–2881.

5 H.T. Kim, M.H. Nam, J.H. Kim, S. Nahm, Microwave dielectric properties and chemical resistance of low-temperature-sintered $CaZrB_2O_6$ ceramics, Int. J. Appl. Ceram. Technol. 6 (5) (2009) 587–592.

6 G.K. Choi, J.R. Kim, S.H. Yoon, K.S. Hong, Microwave dielectric properties of scheelite (A=Ca, Sr, Ba) and wolframite (A=Mg, Zn, Mn) $AMoO_4$ compounds, J. Eur. Ceram. Soc. 27 (2007) 3063–3067.

7 Y.X. Hu, D.M. Wei, Q.Y. Fu, J. Zhao, D.X. Zhou, Preparation and microwave dielectric properties of $3ZnO \cdot B_2O_3$ ceramics with low sintering temperature, J. Eur. Ceram. Soc. 32 (3) (2012) 521–524.

8 S. Garcia-Blanco, J. Fayos, The crystal structure of zinc orthoborate, $Zn_3(BO_3)_2$, Z. Kristallogr. 127 (1−4) (1968) 145–159.

9 M.A. Eidem, B.R. Orton, A. Whitaker, Phase equilibria in the system $ZnO–B_2O_3–SiO_2$ at 950 °C, J. Mater. Sci. 22 (11) (1987) 4139–4143.

10 S.H. Yoon, G.K. Choi, D.W. Kim, S.Y. Cho, K.S. Hong, Mixture behavior and microwave dielectric properties of $(1-x)$ $CaWO_4–xTiO_2$, J. Eur. Ceram. Soc. 27 (2007) 3087–3091.

11 C.F. Shih, W.M. Li, M.M. Lin, C.Y. Hsiao, K.T. Hung, Low-temperature sintered $Zn_2TiO_4:TiO_2$ with near-zero temperature coefficient of resonant frequency at microwave frequency, J. Alloy. Compd. 485 (2009) 408–412.

12 Y.C. Liou, Y.T. Chen, W.C. Tsai, Synthesis of temperature-stable microwave dielectric ceramics $NiNb_2O_6$ with TiO_2 addition, J. Alloy. Compd. 477 (2009) 537–542.

13 L.X. Pang, H. Wang, D. Zhou, X. Yao, A new temperature stable microwave dielectric with low-firing temperature in $Bi_2MoO_6–TiO_2$, J. Alloy. Compd. 493 (2010) 626–629.

14 M. Guo, G. Dou, S.P. Gong, D.X. Zhou, Low-temperature sintered $MgWO_4–CaTiO_3$ ceramics with near-zero temperature coefficient of resonant frequency, J. Eur. Ceram. Soc. 32 (2012) 883–890.

15 G. Dou, D.X. Zhou, M. Guo, S.P. Gong, Low-temperature sintered $Zn_2SiO_4–CaTiO_3$ ceramics with near-zero temperature coefficient of resonant frequency, J. Alloy. Compd. 513 (2012) 466–473.

16 G. Dou, D.X. Zhou, M. Guo, S.P. Gong, Y.X. Hu, Low-temperature sintered $Mg_2SiO_4–CaTiO_3$ ceramics with near-zero temperature coefficient of resonant frequency, J. Mater. Sci.: Mater. Electron. 24 (2013) 1431–1438.

17 C.H. Wei, J.H. Jean, Low-fire processing $(Ca_{1-x}Nd_{2x/3})TiO_3$ microwave ceramics, J. Am. Ceram. Soc. 86 (1) (2003) 93–98.

18 C.C. Huang, J.H. Jean, Low-fire processing of $CaTiO_3$ with $2ZnO–B_2O_3$ glass, Jpn. J. Appl. Phys. 43 (6A) (2004) 3516–3520.

19 R. Ubic, I.M. Reaney, Microwave properties of doped lead pyroniobate, J. Eur. Ceram. Soc. 21 (2001) 2659–2662.

20 R. Ubic, I.M. Reaney, Structure and dielectric properties of lead pyrochlores, J. Am. Ceram. Soc. 85 (10) (2002) 2472–2478.

21 B.W. Hakki, P.D. Coleman, A dielectric resonator method of measuring inductive capacities in the millimeter range, IEEE Trans. Microw. Theory Tech. 8 (4) (1960) 402–410.